The Energetic Significance of Metallophilic Interactions

RESEARCH ARTICLE

The Energetic Significance of Metallophilic Interactions

Qingshu Zheng,[a] Stefan Borsley,[a] Gary S. Nichol,[a] Fernanda Duarte[a],[b] and Scott L. Cockroft*[a]

Abstract: Metallophilic interactions are increasingly recognized as playing an important role in molecular assembly, catalysis, and bio-imaging. However, present knowledge of these interactions is largely derived from solid-state structures and gas-phase computational studies rather than quantitative experimental measurements. Here, we have experimentally quantified the role of aurophilic ($Au^{I}\cdots Au^{I}$), platinophilic ($Pt^{II}\cdots Pt^{II}$), palladophilic ($Pd^{II}\cdots Pd^{II}$) and nickelophilic ($Ni^{II}\cdots Ni^{II}$) interactions in self-association and ligand-exchange processes. All of these metallophilic interactions were found to be too weak to be well-expressed in several solvents. Computational energy decomposition analyses supported the experimental finding that metallophilic interactions are overall weak, meaning that favorable dispersion and orbital hybridization contributions from M···M binding are largely outcompeted by electrostatic or dispersion interactions involving ligand or solvent molecules. This combined experimental and computational study provides a general understanding of metallophilic interactions and indicates that great care must be taken to avoid over-attributing the energetic significance of metallophilic interactions.

Introduction

Metallophilic interactions are often described as occurring in closed shell (d^{10}, s^2) or pseudo-closed shell (d^8) metal···metal contacts.[1] The most well-known and widely reported sub-class of metallophilic interactions are aurophilic interactions, which occur between gold atoms.[1e, 1f, 2] Analogous, although less prevalent, interactions have been reported in other metal-complexes containing Pd(II), Pt(II), Hg(I), Cu(I) and Ag (I) centers.[1e, 1f, 3] Such metallophilic interactions have been suggested to be important for structural control,[4] catalysis,[5] and luminescent and sensing applications.[4d, 6] Despite their potential applications, the nature and strength of these interactions are poorly understood.[7]

Previous quantitative investigations of metallophilic interactions have been largely confined to computational analyses, which have variously ascribed the origin of aurophilic interactions to orbital hybridization, dispersion or relativistic effects.[2-3, 8] Early approaches, employing the Extended Hückel method, suggested orbital mixing between the filled 5*d* and the empty 6*s*/6*p* shells of neighboring metal atoms as the origin of aurophilic and cuprophilic interactions.[3b, 9] At the Hartree-Fock level, the interaction energy curves are repulsive, and the aurophilic attraction only appeared when electron correlation is introduced at the Second-order Møller-Plesset (MP2) perturbation level of theory.[10] This result therefore suggested that dispersion is the dominant attractive component of aurophilic interactions. Subsequently, local MP2 (LMP2) calculations suggested that dispersion and ionic contributions are equally important, and that both of these attractive contributions are dominated by pair-excitations from gold 5*d* orbitals.[11] In contrast, dispersion-corrected density-functional theory calculations suggested that dispersion contributions are much less important than the earlier MP2 calculations had indicated, and also relatively independent of the metal.[12] Instead, the prevalence of gold···gold contacts was attributed to the relativistic enhancement of the electron affinity of gold, thereby preventing gold from forming ionic structures involving bridging anions. Similarly, QCISD and CCSDT approaches also contradict the suggestion from MP2 calculations that metallophilic interactions become more favorable on descending group 11.[13] Most recently, molecular orbital analysis and energy decomposition analysis has suggested that the dimerization of metal complexes arises from a combination of favorable electrostatic interactions and weakly covalent metal···metal orbital interactions, which are counterbalanced by Pauli repulsion.[14]

The theoretical inconsistencies regarding the nature of metallophilic interactions also extend to estimates of their strength; calculated gas-phase energies range from negligible at one extreme,[8b, 8c] to being comparable to hydrogen bonding at the other (*i.e.* 0 to –60 kJ mol^{-1}).[1a, 1e, 1f, 12, 15] Indeed, there is very limited experimental data to support the energetic significance of metallophilic interactions. For example, molecular balance approaches examining the energetics associated with conformational change[16] have been employed to evaluate aurophilic interactions.[17] However, these balances evaluated transition state energy barriers rather than equilibrium conformational free energy differences,[16] meaning that steric factors also contributed to the determined energies. The self-association of metal complexes in solution has been used to experimentally evaluate metallophilic interactions.[18] Most recently, a combined experimental/computational study employing gas-phase collision-induced dissociation experiments confirmed a range of 25–30 kJ mol^{-1} for aurophilic interactions, but the experiments were not amenable to the examination of neutral dimers or interactions in solution.[19] Indeed, it remains challenging to isolate the metallophilic contribution to the overall interaction from other factors, such as the polarizing influences of charged metal centers, interactions between ligands and solvent effects.[20] Thus, the obscure origin of metallophilic interactions, combined with the challenges associated with the evaluation of their strength encouraged us to undertake a solution-phase

[a] Dr Q. Zheng, Dr S. Borsley, Dr G. S. Nichol, Prof. S. L. Cockroft
EaStCHEM School of Chemistry
University of Edinburgh
Joseph Black Building, David Brewster Road, Edinburgh EH9 3FJ, United Kingdom.
E-mail: scott.cockroft@ed.ac.uk

[b] Prof. Dr F. Duarte, Chemistry Research Laboratory
University of Oxford
12 Mansfield Road, Oxford OX1 3TA, United Kingdom.

Supporting information for this article is given via a link at the end of the document.

experimental investigation using minimal synthetic complexes that were amenable to computational analysis.

Here, we have investigated the origin and significance of metallophilic interactions through a combined experimental and computational approach. We synthesized a range of complexes hosting Au(I)···Au(I), Pt(II)···Pt(II), Pd(II)···Pd(II), and Ni(II)···Ni(II) contacts (Figures 1C and 5A). Self-association and ligand-exchange experiments were used to estimate the energetic significance of metallophillic interactions occurring in these complexes (Figures 1, 2 and 5). The energetic contributions in both our experimental systems and several previously reported complexes containing close metal···metal contacts were further analyzed using empirical and computational energy partitioning (Figures 2B, 3, 4 and 5), such that general conclusions on the nature and strength of metallophilic interactions could be drawn.

Results and Discussion

We initiated our study by examining closed shell Au(I)···Au(I) interactions using two complementary approaches: supramolecular self-association[18] (Figure 1A), and ligand-exchange[20] (Figure 1B). These experimental approaches facilitated the respective examination of inter- and intramolecular aurophilic interactions. We reasoned that an ideal model system for assessing the significance of aurophilic contributions should be: (i) an overall neutral complex, to minimize ionic forces, (ii) a gold(I) complex with a closed-shell, d^{10} electronic configuration, (iii) a linear or planar structure with small ligands that allow close contact of the gold centers while minimizing steric effects, (iv) stable and soluble, to enable solution-phase experiments, (v) small enough to be subjected to computational analysis using a range of methods.

Based on the above considerations, complexes **1**–**4** (Figure 1C) were synthesized (Scheme S1). Single-crystal X-ray structures of complexes **2**–**4** showed close Au···Au contacts in the range of 3.3–3.5 Å (Figures S71–S78). These short Au···Au contacts are shorter the pairwise sum of the crystallographically determined van der Waals radii for gold (3.7–4.4 Å),[21] and also lie within the previously reported range for aurophilic interactions (2.8–3.5 Å).[9b, 11] However, the non-planar structure of complex **1** hindered the formation of close Au···Au contacts in the solid state. Nonetheless, complexes **2**–**4** satisfied our ideal design criteria for examining aurophilic interactions. The neutral, linear Au(I) complexes are planar, allowing stacking of the complexes with close Au···Au contacts. The electron-withdrawing pentafluorophenyl group increases the stability of the complexes.[22] Furthermore, the complexes showed good solubility in a range of solvents (Table S1), allowing the behavior of the complexes to be studied in solution by ^{1}H and ^{19}F NMR spectroscopy.

Initially, the self-association (Figure 1A) of complex **2** was investigated. However, neither NMR spectroscopy in acetone-d_6

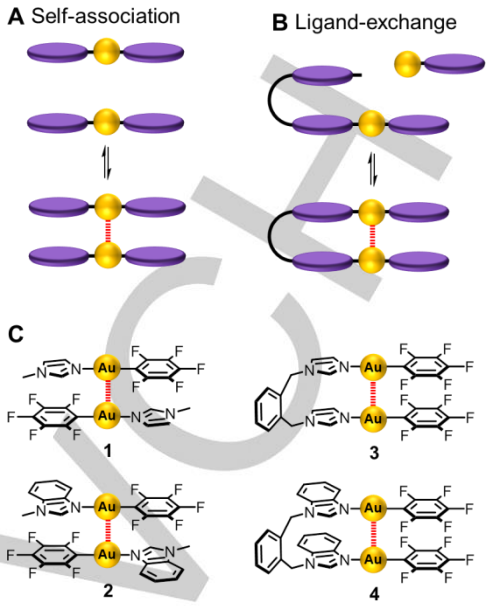

Figure 1. Self-association (**A**) and ligand-exchange (**B**) approaches for assessing aurophilic interactions in solution. Yellow spheres represent metals. Complexes **1**–**4** (**C**) are employed in these two approaches.

(Figures S5–S6) nor UV-vis absorption in dichloromethane (Figure S9) showed any concentration-dependent changes indicative of self-association over concentration ranges spanning 0.001 mM to 22 mM (solubility limit in acetone). While intermolecular aurophilic interactions appeared not to be preserved in solution in this system, we proposed that an intramolecular approach may instead aid the formation of metallophilic interactions that would otherwise be too weak to overcome the entropic penalty associated with intermolecular association.[16, 23] Thus, we designed U-shaped complexes **3** and **4**, where Au···Au contacts are enforced *via* a bridging ligand (Figure 1C).[24] The strength of the intramolecular interactions in these enforced systems may be probed through a ligand-exchange approach, where the intramolecular interactions between two gold fragments influence the equilibrium position (Figure 1B). Complex **4** contains a U-shaped ligand **L$_4$** bound to two identical AuC_6F_5 moieties (Figure 1C). The Au–N bond in these complexes is labile and formed under thermodynamic control, and would be expected to be energetically similar in both complex **2** and complex **4**. Upon mixing ligand **L$_4$** with two equivalents of complex **2**, two equilibria describe the ligand exchange process (Figure 2A). Initially, ligand exchange between ligand **L$_4$** and two equivalents of complex **2** gives rise to complex **4′** while releasing ligand **L$_2$** into solution. A subsequent ligand exchange with another equivalent of complex **2** forms complex **4**, releasing a second molecule of **L$_2$** into solution. Analogous experiments were also performed using ligand **L$_3$** and complex **1** in a wide range of solvents (Figure 2B). Due to the slow exchange of ligands on the NMR timescale, the equilibrium concentrations of all species could be determined by NMR spectroscopy

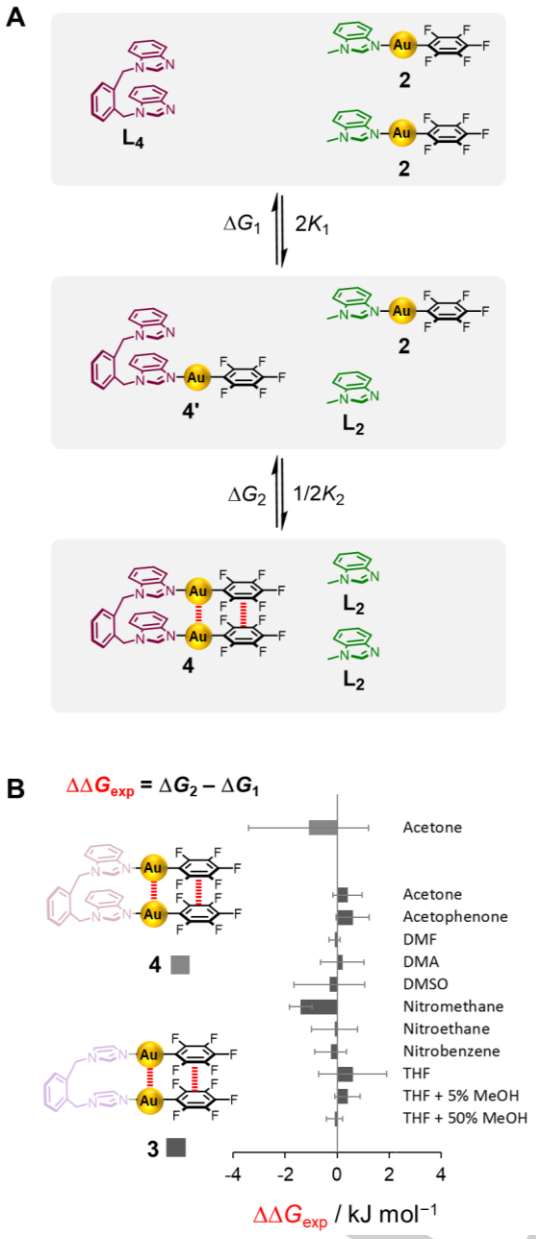

Figure 2. (**A**) Ligand-exchange experiments between complex **2** and ligand $\mathbf{L_4}$ used to examine aurophilic interactions. (**B**) Experimentally determined free energies encompassing aurophilic and aromatic stacking interactions (red dashed lines) between the AuC_6F_5 moieties ($\Delta\Delta G_{exp}$). ^{1}H NMR spectroscopy was used to determine the positions of the equilibria forming complexes **4** (light gray) and **3** (dark gray) at 298K. Experimental errors represent two standard deviations determined from three repeat measurements.

(Figures S1–S20). Therefore, equilibrium constants K_1 and K_2 could be determined from equations (1) and (2) respectively, which account for the statistical factor associated with a 2:1 binding isotherm.[25]

$$2K_1 = \frac{[\mathbf{4'}][\mathbf{L_2}]}{[\mathbf{2}][\mathbf{L_4}]} \quad (1)$$

$$1/2\,K_2 = \frac{[\mathbf{4}][\mathbf{L_2}]}{[\mathbf{2}][\mathbf{4'}]} \quad (2)$$

$$\Delta G_i = -RT\ln K_i \quad i = 1,2 \quad (3)$$

$$\Delta\Delta G = \Delta G_2 - \Delta G_1 \quad (4)$$

The free energy of the equilibria, ΔG, may thus be obtained using equation (3). The difference between ΔG_2 and ΔG_1 (equation (4)) corresponds to the intramolecular interaction energy between the two identical AuC_6F_5 moieties ($\Delta\Delta G_{exp}$), i.e. the sum energy of the aurophilic interactions and the interactions between the pentafluorophenyl rings (Figure 2B).

Thermodynamic control of the equilibrium populations of states depicted in Figure 2A was confirmed by the observation of identical product distributions for both the forward and reverse ligand-exchange experiments, and with equilibrium being established in under 5 minutes (Figures S14–S15). The free energy difference, ΔG_1 was determined to be +1.5 ± 1.6 kJ mol^{-1} in acetone-d_6. This small energy difference indicates that the Au–N coordination bonds in complexes **2** and **4′** are energetically equivalent. Interestingly, ΔG_2 was within error of ΔG_1, with a measured value of +0.4 ± 1.7 kJ mol^{-1}. Therefore, application of equation (4) gave $\Delta\Delta G_{exp}$ = −1.1 ± 2.3 kJ mol^{-1} in acetone-d_6. This negligible value illustrates an absence of either positive or negative cooperativity in the second equilibrium shown in Figure 2. Thus, the sum energy of the aurophilic and stacking interactions between the pentafluorophenyl rings is minor. The same experimental approach was employed with complex **3**, which possessed better solubility, and little variation was observed in the determined $\Delta\Delta G_{exp}$ values in eleven different solvents (Figures 2B, S16–S20).

While the determined $\Delta\Delta G_{exp}$ values were very small, it remained possible that the aurophilic interaction was obscured by electrostatic repulsion between the perfluorinated rings, or other factors that have not been accounted for. Thus, to gain insight into these possibilities, a detailed computational analysis of the system was undertaken. Electrostatic potential surfaces (ESPs) calculated at the M06/LACVP level confirmed the electron-rich nature of the perfluorinated rings due to the formal negative charge on the carbon atom bonded to the gold(I) centers (Figure S23). We next sought a more quantitative analysis of the interactions present within our gold···gold complexes by employing computational energy decomposition analysis (EDA), which enabled interaction energies to be partitioned into the electrostatic, dispersion, orbital and Pauli repulsion components.[26] First, the crystal structure of complex **4** was computationally modified to remove the phenyl ring bridging between each half of the complex, yielding dimer **4a** (Figure 3A, top), which provided an intermolecular analogue of complex **4**. Next, dimer **4b** (Figure 3A, bottom) was attained by computationally replacing the two C_6F_5 moieties in dimer **4a** with hydrogen atoms. EDA calculations were then performed using the ADF2017.110 package at ZORA-PBE-D3BJ/TZ2P, which

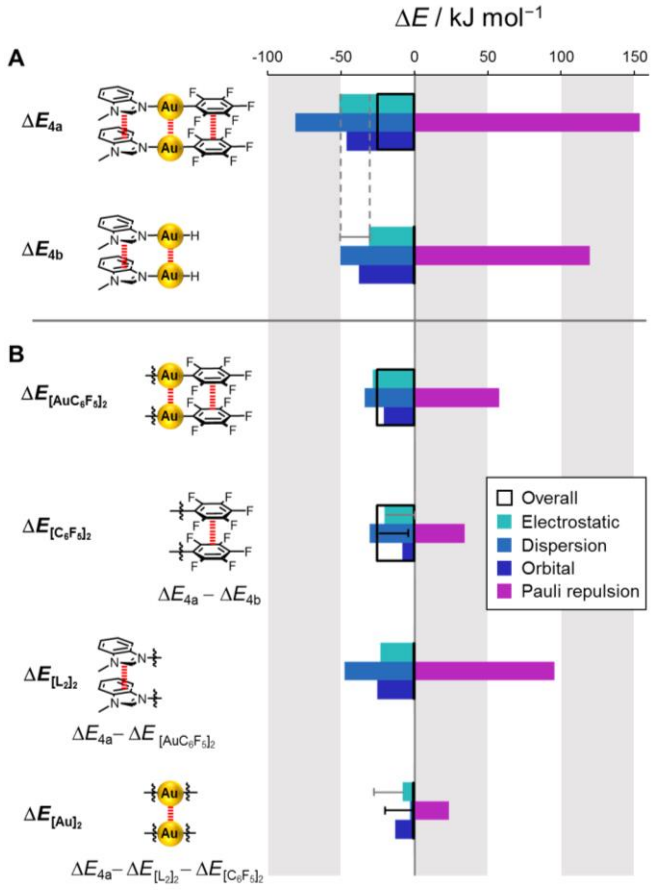

Figure 3. Energy decomposition analysis (EDA) results. The overall interaction energies (hollow black bars) are decomposed into electrostatic (cyan), dispersion (light blue), orbital (dark blue), and Pauli repulsion (magenta) components. (A) EDA calculations were performed on dimers **4a**, **4b**, which are computationally modified structures generated from the crystal structure of **4**. (B) Fragments dissected from complex **4** and dimers **4a** and **4b**. See SI section 5.4 for details, where additional fragments are also presented. Computations were performed using the ADF2017.110 package at ZORA-PBE-D3BJ/TZ2P level. Error bars estimate the maximum non-transferrable attributable error arising from the propagation of electrostatic repulsion between the hydrides in dimer **4b** (*i.e.* the difference between the electrostatic components of ΔE_{4a} and ΔE_{4b}, indicated by vertical dashed lines in A).

accounts for relativistic effects that are known to be important in gold chemistry.[8a, 10, 27] The EDA calculations were performed on dimers **4a** and **4b** without further optimization to avoid distortion of the geometries of the dimers (Figure S22).

The overall interaction energy between the monomers in dimer **4a** was calculated as being comparable to a weak hydrogen bond in the gas phase[23] (black hollow bar in Figure 3, –24.5 kJ energy. Further EDA partitioning provided an estimate of the intermolecular interactions in the **[AuC$_6$F$_5$]$_2$** fragment (Figure 3B and Section 5.4 in the SI). Meanwhile, the energy differences mol^{-1}). The dominant attractive component was determined to be (Figure 3A, top). In comparison, all interaction components were diminished in the dimer **4b**, which had a negligible total interaction dispersion, followed by electrostatic and orbital contributions indicated under the structures in Figure 3B yielded estimates of the intermolecular interaction energies of the **[C$_6$F$_5$]$_2$** and **[L$_2$]$_2$** dimers, and ultimately that of the Au···Au contribution, **[Au]$_2$** (Figure 3B, bottom). Applying the same analysis to the imidazole-derivative **3** (Figure 1) revealed very similar dissected interaction magnitudes (Figure S29). It should be cautioned that such dissected energies are only approximate due to limitations of the partitioning approach.

The replacement of the **C$_6$F$_5$** fragments in **4a** with hydrides in **4b** (Figures 3A) does not significantly change the partial charges on the adjacent benzimidazole ligands (Figure S28), making the dissected intermolecular interaction energy of the **[AuC$_6$F$_5$]$_2$** fragment reasonably reliable. However, the formal negative charge delocalized over each **C$_6$F$_5$** fragment in **4a** are instead localized to the hydride positions in **4b**. Thus, the total electrostatic component of the intermolecular interaction in **4b** is likely to be non-representative of the situation in **4a** due to repulsion between the hydridic positions. The most conservative means of estimating such an error is to attribute the entire difference between the electrostatic interaction energies of **4a** and **4b** as arising from non-transferrable hydridic repulsion, and to propagate this difference through all dependent dissected electrostatic and interaction energies (gray and black error bars in Figure 3, respectively). Even after making such a conservative error estimate, the total energy of the Au···Au interaction is found to be small in comparison to the ligand···ligand interactions that also occur within the dimer complex (Figure 3B, bottom), Consistent with recent examinations of aurophilic [8b, 8c, 28] and stacking interactions,[29] the energy decomposition analysis revealed that dispersion is the dominant attractive component in all of the stacked dimer fragments, but not the **[Au]$_2$** dimer. Instead, the dissection suggests that the main stabilizing forces in the **[Au]$_2$** dimer arise from either electrostatic or orbital interactions. A favorable contribution from orbital interactions in aurophilic interactions is further confirmed by deformation plots generated by the extended transition state method combined with natural orbitals for chemical valence (ETS-NOCV, also called EDA-NOCV, Figures S30–S31). The two dominant NOCVs are both related to the gold centers and contribute about 40% to the total orbital interactions of dimer **4a**, which is in good agreement with both the empirical fragmentation approach presented in Figure 3 and previous EDA-based analyses.[30]

Having examined the nature of aurophilic interactions in intramolecular complexes **3** and **4**, we sought to extend the analysis to other systems. The dimer of complex **2** is chemically identical to dimer **4a**, but with an antiparallel head-to-tail arrangement, rather than parallel head-to-head packing (Figure 4, top). The alternating red/blue colors of the electrostatic potential surface scale show that complex **2** is highly polarized, and thus the head-to-tail, antiparallel stacking is to be expected. Indeed, EDA analysis of the dimer of complex **2** obtained from the crystal structure showed that the interaction holding the dimer together is electrostatically dominated (Figure 4, top right). Significantly,

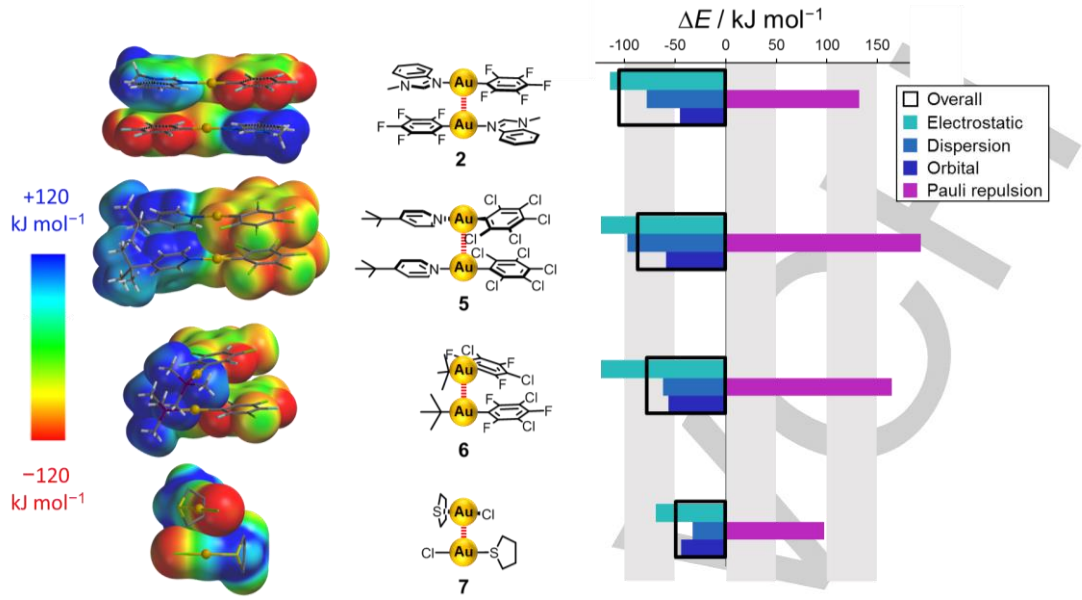

Figure 4. Electrostatic potentials (left) and computed energy decomposition analysis (right) determined from the crystal structures of complex **2** and literature complexes **5**, **6**, and **7**.[22, 31] Electrostatic potential surfaces calculated using M06/LACVP level, and EDA calculations performed using the ADF2017.110 package at ZORA-PBE-D3BJ/TZ2P level.

electrostatic interactions were also found to dominate the dimeric packing modes of literature examples of other Au(I) complexes **5**, **6**, and **7** (Figure 4).[22, 30-31] The dispersion contribution scales qualitatively with the contact area of the dimers. Interestingly, the orbital component is the most consistent across all four species, suggesting that this is a transferrable characteristic of aurophilic interactions. The dominance of electrostatics across all dimers in Figure 4 is noteworthy; complexes **3** and **4** also revealed electrostatically dominated assembly in their extended crystal packing modes (Figure S23), as do several other related complexes.[30] Consistent with the importance of electrostatic interactions in the packing mode, all of these compounds were only soluble in polar organic solvents (Table S1). The overall implications are that electrostatic and dispersion contributions are the dominant factors driving the assembly of most Au(I) complexes, with a weaker orbital mixing contribution involving the metal-metal contacts.

To explore the generality of our finding that aurophilic interactions are weak and are not well-expressed in solution, we extended our investigation to include metallophilic interactions involving group 10 metals. We designed and synthesized complexes **8** and **9**, which incorporate Pt(II), Pd(II) and Ni(II) metal centers (Figure 5A), which could be used to examine metallophilic interactions through a self-association process (Figure 1A). Like the Au(I) complexes examined above, the Ni(II), Pd(II) and Pt(II) complexes were overall neutral. A crystal structure of complex **8-Pt** was obtained, showing dimer formation and close metal···metal contacts in the solid state (Figures S79–S81). Crucially, the thiol ligand on the metal is orientated orthogonally to the plane of the complex, preventing oligomerization into chains and thereby restricting self-association to dimer formation (Figures 5A and S34). The self-association process in solution was monitored by ^{1}H NMR spectroscopy, following concentration-dependent changes in chemical shifts (Figures S35–S39). The chemical shift changes were fitted to a 1:1 binding isotherm, and binding energies were determined using equation (3). The ΔG values obtained were small and ranged between −1 and −5 kJ mol^{-1} (Figure 5B), indicating that the intermolecular interactions between the monomers are not well preserved in solution. Most significantly, there was no systematic change in the association energies in relation to the position of the group 10 metal in the periodic table, further indicating that metallophilic contributions to the total energy were small.

Energy decomposition analysis of the dimers (based on computationally modified crystal structures of **8-Pt**, Figure 5C and Figures S40–S41) revealed the dominant role of electrostatics in dimer formation of complexes **8** and **9**, which was consistent with the earlier results determined for the gold dimers (Figure 4). Significant dispersion and orbital contributions were also determined. A minimal change in the dispersion and orbital contributions was calculated as the metal center was varied, while the electrostatic component increased from Ni to Pd to Pt. This increase is offset by a corresponding decrease in the Pauli repulsion term, resulting in a constant overall interaction energy. The dispersion term is likely to be dominated by the aromatic stacking between the planar aromatic ligands and thus does not change in relation to the metal center. The change in metal affects the electrostatic component slightly, as reflected in subtle

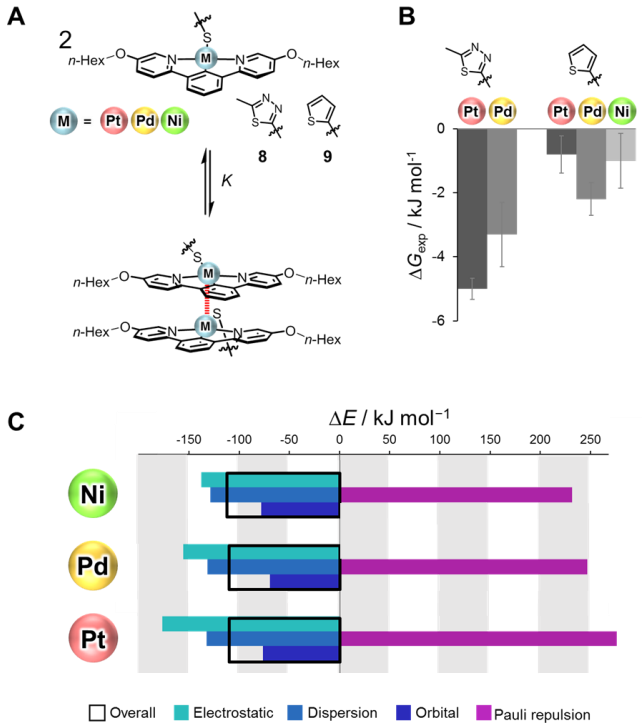

Figure 5. (**A**) Structures and self-association experiments of complexes **8** and **9** used to examine metallophilic interactions. (**B**) Experimentally determined free energies (ΔG) of dimerization, encompassing metallophilic interactions obtained from concentration-dependent ^{1}H NMR spectroscopy in $CDCl_3$ at 298 K. Experimental errors represent two standard deviations determined from three repeat titrations. (**C**) EDA computation results for complex **8** in which the crystal structure of **8-Pt** was computationally modified (Hex replaced by Me and metal center varied, Figures S40–S41). EDA calculations performed using the ADF2017.110 package at the ZORA-PBE-D3BJ/TZ2P level.

variations of the ESP surfaces (Figure S42). As observed for the gold complexes shown in Figure 4, there is little variance in the orbital term in Figure 5 as the metal center is varied from Ni to Pd to Pt in complex **8**. EDA-NOCV plots for the complexes containing the group 10 metals confirmed very small changes in the orbital energies upon varying the metal (Figures S43–S44). Again, this suggests that weakly favorable orbital interactions may be a transferrable general characteristic of metallophilic interactions. Overall, our combined experimental and computational investigation provides a consistent indication that metallophilic interactions are generally weak and therefore overshadowed by interactions involving the ligands or surrounding solvent molecules.

Conclusion

In summary, we have presented a combined experimental and computational investigation into the strength and nature of metallophilic interactions involving aurophilic ($Au^I\cdots Au^I$), platinophilic ($Pt^{II}\cdots Pt^{II}$), palladophilic ($Pd^{II}\cdots Pd^{II}$), and nickelophilic ($Ni^{II}\cdots Ni^{II}$) contacts. Specifically, we have employed a self-assembly approach to study intermolecular metallophilic interactions, and a ligand exchange approach to examine intramolecular interactions. Our experimental results consistently showed that metallophilic interactions in overall neutral complexes are too weak to be well-expressed in solution. The results are supported by computational energy decomposition analysis of both our own experimental systems, and examples from the literature. The computational analyses confirm that metallophilic interactions are indeed weak, and suggest that weakly favorable orbital hybridization contributions are a transferrable characteristic. Our findings in homo-bimetallic complexes may be compared with those obtained for hetero-bimetallic complexes, where electrostatics and orbital interactions were identified as being more important than dispersion in determining metallophilic contacts in the gas-phase.[15] Indeed, our experimental results obtained in solution are consistent with weakly favorable metal···metal contacts being eclipsed by electrostatic and dispersion interactions involving the surrounding ligands and solvent.[8c] The importance of electrostatic interactions and solvent effects in the assembly of metallophilic complexes is underscored by the prevalence of head-to-tail crystal packing (*e.g.* Figure 4),[30] the solubility of complexes bearing smaller organic ligands being limited to polar organic solvents (*e.g.* Table S1), and the (solvophobic) stabilization of "metallophilic" stacks in the presence of cohesive solvents such as water and methanol (Table S1).[18, 32] Thus, in view of the other major energetic contributors, caution must be exercised to avoid overestimating the significance of metallophilic interactions based solely on the observation of short metal-metal contacts.

Experimental Section

Experimental details including synthetic details, characterization data, experimental data and analysis, computational details are provided in the Supporting Information. Single-crystal X-ray structure CCDC deposition codes: 1894944–1894951.Acknowledgements

We thank Dr Lorna Murray for assistance with NMR spectroscopy, and the China Scholarship Council for funding to QZ.

Keywords: Metal-metal interactions • Noncovalent interactions • Metallophilic interactions • Supramolecular chemistry • Computational chemistry

[1] a) S. Sculfort, P. Braunstein, *Chem. Soc. Rev.* **2011**, *40*, 2741-2741; b) P. Pyykkö, *Chem. Rev.* **1997**, *97*, 597-636; c) H. Schmidbaur, A. Schier, *Organometallics* **2015**, *34*, 2048-2066; d) H. Schmidbaur, A. Schier, *Angew. Chem. Int. Ed.* **2015**, *54*, 746-784; *Angew. Chem.* **2015**, *127*, 756-797; e) H. Schmidbaur, A. Schier, *Chem. Soc. Rev.* **2012**, *41*, 370-412; f) H. Schmidbaur, A. Schier, *Chem. Soc. Rev.* **2008**, *37*, 1931-1951.

[2] P. Pyykkö, *Angew. Chem. Int. Ed.* **2004**, *43*, 4412-4456; *Angew. Chem.* **2004**, *116*, 4512-4557.

[3] a) E. Hupf, R. Kather, M. Vogt, E. Lork, S. Mebs, J. Beckmann, *Inorg. Chem.* **2016**, *55*, 11513-11521; b) P. K. Mehrotra, R. Hoffmann, *Inorg. Chem.* **1978**, *17*, 2187-2189; c) K. Singh, J. R. Long, P. Stavropoulos, *J. Am. Chem. Soc.* **1997**, *119*, 2942-2943.

[4] a) M. J. Katz, K. Sakai, D. B. Leznoff, *Chem. Soc. Rev.* **2008**, *37*, 1884-1895; b) A. Deák, T. Megyes, G. Tárkányi, P. Király, L. Biczók, G. Pálinkás, P. J. Stang, *J. Am. Chem. Soc.* **2006**, *128*, 12668-12670; c) U. E. I. Horvath, J. M. McKenzie, S. Cronje, H. G. Raubenheimer, L. J.

Barbour, *Chem. Commun.* **2009**, 6598-6600; d) J. C. Vickery, M. M. Olmstead, E. Y. Fung, A. L. Balch, *Angew. Chem. Int. Ed. Engl.* **1997**, *36*, 1179-1181; *Angew. Chem.* **1997**, *109*, 1227-1229.

[5] a) E. Tkatchouk, N. P. Mankad, D. Benitez, W. A. Goddard, F. D. Toste, *J. Am. Chem. Soc.* **2011**, *133*, 14293-14300; b) M. H. Larsen, K. N. Houk, A. S. K. Hashmi, *J. Am. Chem. Soc.* **2015**, *137*, 10668-10676; c) D. Weber, M. R. Gagné, *Top Curr. Chem.* **2015**, *357*, 167-212; d) E. S. S. Smirnova, A. M. Echavarren, *Angew. Chem. Int. Ed.* **2013**, *52*, 9023-9026; *Angew. Chem.* **2013**, *125*, 9193-9196.

[6] a) K. M. C. Wong, V. W. W. Yam, *Acc. Chem. Res.* **2011**, *44*, 424-434; b) V. W.-W. Yam, E. C.-C. Cheng, *Chem. Soc. Rev.* **2008**, *37*, 1806-1806; c) C.-M. Che, M.-C. Tse, M. C. W. Chan, K.-K. Cheung, D. L. Phillips, K.-H. Leung, *J. Am. Chem. Soc.* **2000**, *122*, 2464-2468; d) A. Kishimura, T. Yamashita, T. Aida, *J. Am. Chem. Soc.* **2005**, *127*, 179-183; e) M. C.-L. Yeung, V. W.-W. Yam, *Chem. Soc. Rev.* **2015**, *44*, 4192-4202; f) M. A. Mansour, W. B. Connick, R. J. Lachicotte, H. J. Gysling, R. Eisenberg, *J. Am. Chem. Soc.* **1998**, *120*, 1329-1330.

[7] P. Hobza, J. Řezáč, *Chem. Rev.* **2016**, *116*, 4911-4912.

[8] a) H. Schmidbaur, S. Cronje, B. Djordjevic, O. Schuster, *Chem. Phys.* **2005**, *311*, 151-161; b) M. Andrejić, R. A. Mata, *Phys. Chem. Chem. Phys.* **2013**, *15*, 18115-18122; c) A. Wuttke, M. Feldt, R. A. Mata, *J. Phys. Chem. A* **2018**, *122*, 6918-6925.

[9] a) Y. Jiang, S. Alvarez, R. Hoffmann, *Inorg. Chem.* **1985**, *24*, 749-757; b) L. F. Veiros, M. J. Calhorda, *J. Organomet. Chem.* **1996**, *510*, 71-81; c) D. G. Evans, D. M. P. Mingos, *J. Organomet. Chem.* **1985**, *295*, 389-400.

[10] P. Pyykkö, Y. Zhao, *Angew. Chem. Int. Ed. Engl.* **1991**, *30*, 604-605; *Angew. Chem.* **1991**, *103*, 622-623.

[11] N. Runeberg, M. Schütz, H.-J. J. Werner, *J. Chem. Phys.* **1999**, *110*, 7210-7215.

[12] A. Otero-De-La-Roza, J. D. Mallory, E. R. Johnson, *J. Chem. Phys.* **2014**, *140*.

[13] E. O'Grady, N. Kaltsoyannis, *Phys. Chem. Chem. Phys.* **2004**, *6*, 680-687.

[14] M. B. Brands, J. Nitsch, C. F. Guerra, *Inorg. Chem.* **2018**, *57*, 2603-2608.

[15] E. Paenurk, R. Gershoni-Poranne, P. Chen, *Organometallics* **2017**, *36*, 4854-4863.

[16] I. K. Mati, S. L. Cockroft, *Chem. Soc. Rev.* **2010**, *39*, 4195-4205.

[17] a) H. Schmidbaur, W. Graf, G. Müller, *Angew. Chem. Int. Ed. Engl.* **1988**, *27*, 417-419; *Angew. Chem.* **1988**, *100*, 439-441; b) H. Schmidbaur, K. Dziwok, A. Grohmann, G. Müller, *Chem. Ber.* **1989**, *122*, 893-895; c) D. E. Harwell, M. D. Mortimer, C. B. Knobler, F. A. L. L. Anet, M. F. Hawthorne, *J. Am. Chem. Soc.* **1996**, *118*, 2679-2685.

[18] R. Gavara, E. Aguiló, C. F. Guerra, L. Rodríguez, J. C. Lima, *Inorg. Chem.* **2015**, *54*, 5195-5203.

[19] E. Andris, P. C. Andrikopoulos, J. Schulz, J. Turek, A. Růžička, J. Roithová, L. Rulíšek, *J. Am. Chem. Soc.* **2018**, *140*, 2316-2325.

[20] E. Hartmann, R. M. Gschwind, *Angew. Chem. Int. Ed.* **2013**, *52*, 2350-2354; *Angew. Chem.* **2013**, *125*, 2406-2410.

[21] a) J. Muñiz, C. Wang, P. Pyykkö, *Chem. Eur. J.* **2011**, *17*, 368-377; b) S. S. Batsanov, *Experimental foundations of structural chemistry*, Moscow University Press, **2008**.

[22] E. J. Fernández, A. Laguna, J. M. López-de-Luzuriaga, M. Monge, M. Montiel, M. E. Olmos, J. Pérez, M. Rodríguez-Castillo, *Gold Bull.* **2007**, *40*, 172-183.

[23] C. A. Hunter, *Angew. Chem. Int. Ed.* **2004**, *43*, 5310-5324; *Angew. Chem.* **2004**, *116*, 5424-5439.

[24] Dilution experiments of complex **3** also showed no evidence of intermolecular self-association via aurophilic interactions (Figures S7–S8).

[25] C. A. Hunter, H. L. Anderson, *Angew. Chem. Int. Ed.* **2009**, *48*, 7488-7499; *Angew. Chem.* **2009**, *121*, 7624-7636.

[26] a) K. Morokuma, *J. Chem. Phys.* **1971**, *55*, 1236-1244; b) T. Ziegler, A. Rauk, *Inorg. Chem.* **1979**, *18*, 1558-1565; c) T. Ziegler, a. Rauk, *Theoret. Chim. Acta (Berl.)* **1977**, *46*, 1-10.

[27] E. van Lenthe, J. G. Snijders, E. J. Baerends, *J. Chem. Phys.* **1996**, *105*, 6505-6516.

[28] R. Pollice, P. Chen, *Angew. Chem. Int. Ed.* **2019**, DOI: 10.1002/anie.201905439; *Angew. Chem.* **2019**, DOI: 10.1002/ange.201905439.

[29] L. Yang, J. B. Brazier, T. A. Hubbard, D. M. Rogers, S. L. Cockroft, *Angew. Chem. Int. Ed.* **2016**, *55*, 912-916; *Angew. Chem.* **2016**, *128*, 924-928.

[30] B. Pinter, L. Broeckaert, J. Turek, A. Růžička, F. de Proft, *Chem. Eur. J.* **2014**, *20*, 734-744.

[31] a) T. Lasanta, J. M. Lõpez-de-Luzuriaga, M. Monge, M. E. Olmos, D. Pascual, *Chem. Eur. J.* **2013**, *19*, 4754-4766; b) S. Ahrland, K. Dreisch, B. Norén, Å. Oskarsson, *Mater. Chem. Phys.* **1993**, *35*, 281-289.

[32] a) A. Aliprandi, M. Mauro, L. de Cola, *Nat. Chem.* **2015**, *8*, 10; b) L. Yang, C. Adam, S. L. Cockroft, *J. Am. Chem. Soc.* **2015**, *137*, 10084-10087; c) B. Kemper, L. Zengerling, D. Spitzer, R. Otter, T. Bauer, P. Besenius, *J. Am. Chem. Soc.* **2018**, *140*, 534-537.

Entry for the Table of Contents

RESEARCH ARTICLE

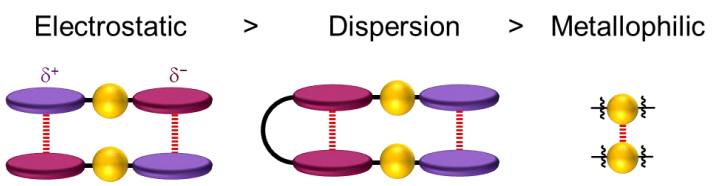

Metallophilic interactions have been widely implicated in governing a range of assemblies, despite a limited, and often contradictory understanding. Here, our combined experimental and computational study provides a general understanding of the nature of metallophilic interactions, and indicates that great care must be taken to avoid over-attributing the energetic significance of metallophilic interactions, particularly in solution.

*Qingshu Zheng, Stefan Borsley, Gary S. Nichol, Fernanda Duarte and Scott L. Cockroft**

Page No. – Page No.

Fool's gold (and silver, nickel, platinum and palladium)